ISSN 0023-1584, Kinetics and Catalysis, 2010, Vol. 51, No. 2, pp. 255–265. © Pleiades Publishing, Ltd., 2010.
Original Russian Text © D.I. Slovetskii, E.M. Chistov, 2010, published in Kinetika i Kataliz, 2010, Vol. 51, No. 2, pp. 270–280.

Catalytic Processes on Membrane Palladium Alloys: I. Carbon Monoxide Disproportionation

D. I. Slovetskii and E. M. Chistov

Topchiev Institute of Petrochemical Synthesis, Russian Academy of Sciences, Moscow, 119991 Russia
e-mail: slovetsk@ips.ac.ru

Received March 4, 2008; in final form, August 6, 2009

Abstract—The results of a kinetic study of the disproportionation reaction of carbon monoxide on the surface of B1–B3 palladium alloy membranes over wide ranges of residence times and temperatures are reported. The specific rates and activation energies of the reaction with the formation of CO_2 and atomic carbon adsorbed on the surface were determined. It was found that the rate of reaction on all of the alloys from the B series other than B3-2 was independent of the consumption of CO and the residence time. The catalytic activity of multicomponent palladium alloy membranes in the CO disproportionation reaction was much lower and the activation energy was higher than the corresponding parameters of Pd–(6–10)Ru and Pd–5.5Ni binary alloy membranes. Atomic carbon formed in the reaction on all of the alloys from the B series other than the B3-2 alloy did not form carbon deposits as polymer films, pyrolytic carbon, or soot strongly bound to the surface of each other to result in a decrease in the rate of reaction. On the surface of the B3-2 alloy, atomic carbon initiated the formation of a polymer film weakly bound to the surface, which decreased the rate of reaction. A reaction mechanism was proposed to adequately describe the experimental results.

DOI: 10.1134/S002315841002014X

INTRODUCTION

The recovery of hydrogen from various gas mixtures, including synthesis gas prepared by hydrocarbon conversion, using palladium alloy membranes is an efficient currently available technique for the production of high-purity hydrogen [1–4]. At the same time, palladium alloy membranes can serve as catalysts for the hydrogenation of carbon oxides and the dehydrogenation of hydrocarbons, alcohols, and ethers [5–9]. Thus, in the extraction of pure hydrogen from the synthesis gas of hydrocarbon conversion with membranes of promising multicomponent palladium alloys, soot formation was observed on the surfaces of membranes, membrane module units, hydrogen flow lines, and lines for the removal of depleted synthesis gas [10]. Moreover, it was experimentally found that, upon passing pure carbon monoxide through a quartz reactor with membrane samples of B1 and B2 alloys and a number of construction materials (St3 and Kh18N10T steels, PSR-72 and PMF-8 solder alloys, nickel, copper, and Pyrex), the disproportionation of CO (Boudoir reaction) occurred at 873 K [10]:

$$2CO \xrightarrow{S_i} CO_2 + C, \qquad (I)$$

which was accompanied by soot formation, especially intensive on St3 steel, nickel, and PSr-72 solder alloy. The strong dependence of the yield of CO_2 on the material of samples at the same parameters (gas pressure and temperature) suggests the heterogeneous character of reaction (I).

The disproportionation reaction was studied on binary alloy membranes in a flow of CO or a mixture of CO with hydrogen [7–9]. In the mixture, the hydrogenation of CO molecules to form C_1–C_2 hydrocarbon and water molecules occurred along with a decrease in the rate of reaction (I). Water molecules can compete with hydrogen molecules in adsorption at the same active surface sites [11] to decrease the rate of formation of CO_2 in reaction (I) and enter into the water gas reaction with CO molecules

$$H_2O + CO \leftrightarrow CO_2 + H_2 \qquad (II)$$

to increase the yield of CO_2.

Thus, to interpret the results of a study of the simultaneous occurrence of all of the above reactions in mixtures of CO with hydrogen, including mixtures prepared by hydrocarbon conversion [1, 4], the disproportionation reaction should be initially studied on palladium alloy membranes in pure CO; then, the water gas reaction and the hydrogenation of CO should be studied.

This work is the first stage of a study of catalytic reactions on multicomponent B series (B1–B3) palladium alloy membranes, which are widely used in the extraction of pure hydrogen from hydrocarbon conversion gas mixtures [1–4]. The aim of this work was to experimentally study the rate of the disproportionation reaction in a flow of pure CO over the working temperature range (573–925 K) in order to predict the maximum possible rate of reaction and to minimize

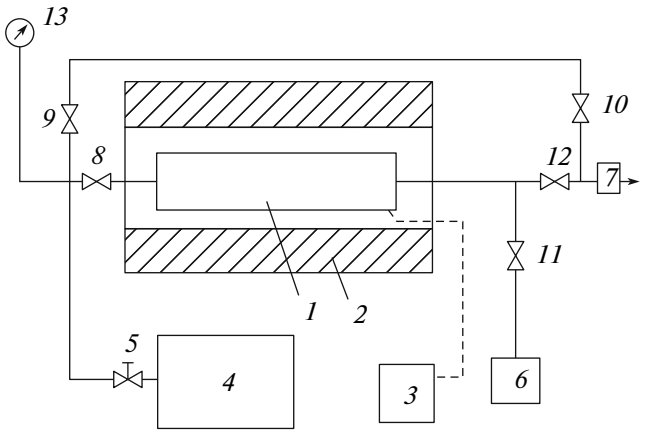

Fig. 1. Experimental setup: (*1*) reactor; (*2*) electric heater; (*3*) temperature measurement and control unit; (*4*) CO preparation, purification, and drying unit; (*5*) regulating valve; (*6*) chromatograph; (*7*) flow meter; (*8–12*) shutoff valves; and (*13*) pressure-and-vacuum gage for measuring gas pressure in the reactor.

the rate of product (primarily, soot) formation in the membrane extraction of pure hydrogen.

EXPERIMENTAL

Experiments were performed in a system (Fig. 1) analogous to that described previously [10], but over wider ranges of temperatures (573–925 K) and membrane alloy compositions. The system included a fused-silica cylindrical flow reactor *1* with an inner diameter of 1.03×10^{-2} m and 70×10^{-2} m long, which was heated with an electric heater *2*, a temperature control and measurement unit *3*, a unit for the generation of CO by the decomposition of formic acid in accordance with a published procedure [12] in the presence of phosphoric acid (H_3PO_4) with chemical gas purification and drying with phosphorus pentoxide at 193 K *4*, a regulation valve *5* arranged in the gas supply line before the reactor inlet for gas flow regulation, an LKhM 8MD chromatograph *6*, and a gas flow meter *7*. The heated lines were made of copper tubes. The reactor temperature was measured using a Chromel–Alumel thermocouple arranged at the outer surface of the reactor wall to exclude a contribution from reaction on the thermocouple surface. The gas flow rate was measured by leakage into calibrated 1- or 5-l volumes, which were preevacuated with a fore vacuum pump, with the automatic detection of the time of pressure increase from initial (~150 Torr) to final values (170–200 Torr) using a Sapfir gage. Gas flow meter *7* allowed us to measure the flow rates of CO immediately at the outlet of valve *5* or a gas mixture at the reactor outlet; for this purpose, shutoff valves *8–12* were mounted in gas inlet and outlet lines. The gas mixture composition at the reactor outlet was determined using chromatograph *6* equipped with the ECOCHROM software for the measurement and processing of chromatograms on a personal computer. High-purity argon or helium was used as the carrier gas in the chromatograph at a flow rate of 1 l/h. Zeolite NaX or Porapak served as sorbents (column length, 2 m; column temperature, 60°C). The chromatograph was calibrated against gases and calibration mixtures at room temperature and atmospheric pressure. To pump CO and products through the reactor, chromatograph, and the measuring system, a small excess pressure was sufficient (p = 0.105 MPa). The gas from the flow meter was supplied to a burner mounted in an exhaust hood and combusted.

Errors in concentration measurements were no higher than ±3% (CO) or ±5% (CO_2) and in gas flow rate measurements, ±5%.

The reactor was filled in turn with the following palladium alloy membranes (wt %):

B1 (Pd–15.6Ag–3.06Au–0.6Pt–0.6Ru–0.24Al);

B2 (Pd–15Ag–1.5In–0.5Y)[10];

B3-1 (Pd–15Ag–1.5In–0.2Y–0.5 W);

B3-2 (Pd–15Ag–1.5In–0.2Y–0.5 Ta);

B3-3 (Pd–15Ag–1.5In–0.2Y–0.5Nb);

B3-4 (Pd–15Ag–1.5In–0.2Y– 0.5Mo) [13].

The B1 alloy was used as a bundle of capillary tubes with an outer diameter of 0.245×10^{-2} m, a wall thickness of 120 μm, and a length of 0.275 ± 0.005 m, and the other alloys were used as the bundles of wire 0.05×10^{-2} m in diameter and from 0.15 to 0.18 m in length (Table 1, columns 1–7), which were degreased, washed with hydrocarbon solvents, and dried. The length of alloy elements was responsible for the length of the active reaction zone (L_r). The bundle of capillary tubes of the B1 alloy more or less uniformly filled the reactor cross section ($S_r = 0.833 \times 10^{-4}$ m^2), and the bundles of wire of the other alloys were chaotically arranged at the bottom to fill less than 5% of the reactor cross section. The surface roughness of alloy samples, which were made by extrusion and broaching, was less than 1%.

Before being charged, the reactor was heated to 873 K and purged with pure dry carbon monoxide at a rate of 0.003 mol/h. In this case, the concentration of CO_2 measured at the reactor outlet at the silica-wall surface area of 0.0227 m^2 was no higher than 0.01%; this demonstrated the low catalytic activity of fused silica (0.67×10^{-5} mol m^{-2} h^{-1}). After loading the reactor with a test material, the required flow rate of CO was adjusted and measured at the pressure p = 0.105 MPa and T = 300 K. Then, the reactor was heated to 873 K, and the presence of impurities in a flow of CO after the outlet of the reactor filled with alloy samples was checked at T = 873 K and minimum flow rates (0.003–0.006 mol/h). The products were analyzed by chromatography with the use of high-purity argon as the carrier gas and a Porapak column for the determination of hydrogen, CO, and CO_2. Only the peaks of CO and CO_2 were detected on Pora-

Table 1. Reactor parameters for studying the kinetics of reactions on various membrane alloys

Alloy	$L_r \times 10^2$, m	$V_r \times 10^6$, m^3	$V_{alloy} \times 10^6$, m^3	$S_{alloy} \times 10^4$, m^2	$V_r - V_{alloy} \times 10^6$, m^3	$\frac{S_{alloy}}{V_r - V_{alloy}} \times 10^{-2}$, m^{-1}
B1	27.5	22.9	1.20	403	21.7	18.6
B2	14.6	12.2	0.50	39.7	11.7	3.4
B3-1	15.9	13.2	0.80	61.5	12.4	5.0
B3-2	18.0	15.0	0.70	56.0	14.3	3.9
B3-3	15.3	12.7	0.80	62.3	11.9	5.2
B3-4	16.2	13.5	0.73	58.3	12.8	4.9
$(\Delta x/x)$, %	±3	±3	±5	±10	±3.5	±15

pak. Because the peak of nitrogen overlapped with the peak of CO because of the same retention times, the measurements were repeated on a column with zeolite, on which the peaks of hydrogen, nitrogen, oxygen, and methane were not detected. The upper estimates of component concentrations with the use of experimental detection sensitivity values were $\ll 0.001\%$ hydrogen and $\ll 0.01\%$ nitrogen and oxygen at the concentrations $C_{CO_2} = 0.5–2.5$ vol %. Consequently, the rate of formation of CO_2 by the oxidation of CO with water vapor and residual oxygen

$$CO + O_2 \longrightarrow CO_2 + O \qquad \text{(III)}$$

was much lower than the rate of formation of CO_2 in reaction (I) so that reactions (II) and (III) can be ignored.

The disproportionation kinetics was studied over a wide ranges of parameters ($T = 573–925$ K and gas flow rates of 0.0022–0.0670 mol/h). Low CO_2 concentrations were measured chromatographically using Porapak columns and helium as the carrier gas. In the course of these experiments, the concentrations C_{CO_2} and C_{CO} at the reactor outlet were calculated from chromatograms. The measured concentrations of CO_2 were corrected for CO_2 formation at the wall surface of the silica reactor. From the refined values of the concentration C_{CO_2} and measured CO flow rates, the specific rate of reaction (I) on the membrane palladium alloy was calculated as a function of temperature and residence time (τ):

$$w_r(T,\tau) = \{C_{CO_2}(T,\tau)Q_{CO}(T,\tau)\}/S_{alloy}, \qquad (1)$$

where C_{CO_2} is the concentration of CO_2 molecules, mole fractions (henceforth, S_{alloy} is the geometric surface area of an alloy sample (Table 1, column 5)). Errors in the calculated absolute values of $\Delta w_r/w_r$ were ±20 and ±10% in the relative values (at $S_{alloy} = \text{const}$).

The tentative gas residence time (τ) with the surface of alloy samples at constant loading, temperature, and pressure was calculated from the measured rate (Q_{CO}) at the reactor outlet and the difference between the volumes of the reaction zone (V_r) and alloy samples (V_{alloy}) (Table 1, columns 3, 4, and 6) using the equation

$$\tau = (V_r - V_{alloy})/\{Q_{CO}(p_0/p)(T/T_0)\}, \qquad (2)$$

where $p_0 = 0.1$ MPa, $T_0 = 273$ K, and p and T are the gas pressure and temperature in the reactor, respectively. Error in the determination of τ was ±8.5%. At a constant length (L_r) of the active reactor zone ($V_r - V_{alloy} = \text{const}$), the residence time was inversely proportional to gas flow rate.

Upon measuring the dependence of the concentration of CO_2 on the flow rate of CO at $T = 873$ K, the reactor temperature was varied at a constant flow rate of CO and the temperature dependence of the concentration of CO_2 in the flow at the reactor outlet and the rate of reaction was obtained.

After completion of measurements in the first sample, the CO drying agent was regenerated at the outlet of reactor *4*, the next sample was loaded, and a cycle of the above measurements and calculations was repeated in turn with the other membrane alloy samples.

RESULTS

Table 2 summarizes the CO_2 concentrations measured at the reactor outlet depending on the rate Q_{CO} at the inlet and calculated using Eq. (1), as well as the specific rates of reaction on various membrane alloys at 873 K. The specific rate of reaction reached a minimum on the B1 alloy and increased in the following order: B1 ⟶ B3-4 ⟶ B3-3 ⟶ B3-1 ⟶ B2 ⟶ B3-2. As the temperature was decreased, it monotonically decreased on all of the alloys (Table 3).

Form the measured temperature dependence of the specific rate in the Arrhenius coordinates, the activation energies of the disproportionation reaction were calculated. The experimental points lied in straight lines (Figs. 2a, 2b) within the limits of relative error for all of the multicomponent membrane alloys, which was $\Delta \log w_r / \log w_r < \pm 7\%$. For comparison, Fig. 2b (lines *7*, *8*) shows the same dependences for Pd–10Ru and Pd–5.5Ni binary membrane alloys calculated

Table 2. Dependence of the concentration of CO_2 and the rate of CO disproportionation on membrane alloys on the gas flow rate at the reactor inlet at $T = 873$ K and $p = 0.105$ MPa

B1			B2			B3-1		
Q_{CO}, mol/h	C_{CO_2}, vol %	$w_r \times 10^3$, mol m^{-2} h^{-1}	Q_{CO}, mol/h	C_{CO_2}, vol %	$w_r \times 10^3$, mol m^{-2} h^{-1}	Q_{CO}, mol/h	C_{CO_2}, vol %	$w_r \times 10^3$, mol m^{-2} h^{-1}
0.0500	0.08	1.00	0.0360	0.17	15.4	0.066	0.16	17.1
0.0300	0.18	1.34	0.0170	0.37	15.6	0.044	0.18	12.8
0.0280	0.19	1.32	0.0120	0.51	15.4	0.026	0.27	11.4
0.0200	0.33	1.64	0.0080	0.77	15.6	0.015	0.45	11.1
0.0140	0.53	1.81	0.0057	1.13	16.1	0.014	0.56	12.7
0.0086	0.78	1.69	0.0047	1.35	15.9	0.010	0.86	14.0
0.0062	0.96	1.49	0.0044	1.49	16.6	0.005	1.72	14.0
			0.0039	1.65	16.1	0.003	2.50	12.2
			0.0034	1.77	15.1			
$\bar{w}_r \times 10^3$ mol m^{-2} h^{-1}		1.55 ± 0.14			15.80 ± 0.39			12.60 ± 0.90
molecule cm^{-2} s^{-1}		2.6×10^{13}			2.6×10^{14}			2.1×10^{14}
		$\sigma^2 = 0.04$			$\sigma^2 = 0.23$			$\sigma^2 = 1.3$
B3-2			B3-3			B3-4		
Q_{CO}, mol/h	C_{CO_2}, vol %	$w_r \times 10^3$, mol m^{-2} h^{-1}	Q_{CO}, mol/h	C_{CO_2}, vol %	$w_r \times 10^3$, mol m^{-2} h^{-1}	Q_{CO}, mol/h	C_{CO_2}, vol %	$w_r \times 10^3$, mol m^{-2} h^{-1}
0.0340	0.50	30.4	0.0630	0.04	4.01	0.0140	0.14	3.43
0.0190	0.94	32.0	0.0130	0.20	4.17	0.0110	0.16	3.09
0.0140	1.13	28.2	0.0110	0.23	4.01	0.0099	0.20	3.43
0.0085	1.44	21.8	0.0093	0.28	4.65	0.0074	0.23	2.92
0.0048	2.14	18.4	0.0079	0.31	3.85	0.0056	0.31	2.92
0.0038	2.50	17.0	0.0066	0.41	4.33	0.0039	0.39	2.57
			0.0041	0.56	3.69	0.0037	0.45	2.92
			0.0036	0.66	3.85	0.0031	0.54	2.92
			0.0032	0.73	3.85			
$\bar{w}_r \times 10^3$ mol m^{-2} h^{-1}		30.2 ± 2.4			4.05 ± 0.22			3.03 ± 0.22
molecule cm^{-2} s^{-1}		5.1×10^{14}			6.8×10^{13}			5.1×10^{13}
		$\sigma^2 = 3.6$			$\sigma^2 = 0.05$			$\sigma^2 = 0.8$
		($n = 3$)						
		14.8 ± 1.0						
		$\sigma^2 = 157$						
		($n = 6$)						

based on published data [7–9, 14]. In these cases, relative errors were greater: ±12% for Pd–5.5Ni and ±20% for Pd–(6–10)Ru. The activation energies of the reaction of CO disproportionation varied from 15 to 95 kJ/mol for multicomponent alloys from the series of B1–B3 and from 9 (Pd–5.5Ni) to 18 kJ/mol (Pd–(6–10)Ru) for two-component alloys (Table 4).

The calculated Reynolds numbers (characterizing turbulence) for all of the alloy samples over the tested range of parameters varied from 0.2 to 4.2, and additional turbulization did not occur in the longitudinal flow around long smooth samples. Thus, the gas flow in the reactor was laminar. The experimental data (Tables 2, 3) in combination with reactor and sample

Table 3. Dependence of the concentration and the rate of formation of CO_2 on the surface temperature of membrane alloys at $p = 0.105$ MPa and constant CO flow rates

B1; $Q_{CO} = 0.0280$ mol/h			B2; $Q_{CO} = 0.0077$ mol/h			B3-1; $Q_{CO} = 0.0260$ mol/h		
T, K	C_{CO_2}, vol %	$w_r \times 10^3$, mol m^{-2} h^{-1}	T, K	C_{CO_2}, vol %	$w_r \times 10^3$, mol m^{-2} h^{-1}	T, K	C_{CO_2}, vol %	$w_r \times 10^3$, mol m^{-2} h^{-1}
751	0.062	0.43	743	0.26	5.04	783	0.055	2.32
767	0.103	0.72	763	0.29	5.62	802	0.06	2.50
770	0.117	0.81	794	0.38	7.34	825	0.13	5.50
790	0.128	0.89	829	0.56	10.90	853	0.21	8.88
810	0.150	1.04	851	0.77	14.90	863	0.21	8.88
841	0.165	1.15	870	0.80	15.50	873	0.24	10.15
873	0.193	1.34	873	0.80	15.50	883	0.29	12.26
			892	0.87	16.90			
			921	1.00	19.40			
B3-2; $Q_{CO} = 0.020$ mol/h			B3-3; $Q_{CO} = 0.048$ mol/h			B3-4; $Q_{CO} = 0.011$ mol/h		
T, K	C_{CO_2}, vol %	$w_r \times 10^3$, mol m^{-2} h^{-1}	T, K	C_{CO_2}, vol %	$w_r \times 10^3$, mol m^{-2} h^{-1}	T, K	C_{CO_2}, vol %	$w_r \times 10^3$, mol m^{-2} h^{-1}
573	0.35	12.50	754	0.075	0.58	793	0.09	1.52
623	0.46	16.43	824	0.272	2.03	836	0.12	2.19
646	0.53	18.92	847	0.375	2.89	873	0.16	3.24
741	0.72	25.71	873	0.518	3.99	924	0.25	4.76
803	0.83	29.64	883	0.572	4.41			
853	0.92	32.86						
873	1.07	38.21						

Pd–10 Ru [8, 9]		Pd–5.5 Ni [8, 9]		Pd–(6, 10) Ru [7, 16]		Pd–5.5 Ni [7, 16]	
T, K	$w_r \times 10^3$, mol m^{-2} h^{-1}	T, K	$w_r \times 10^3$, mol m^{-2} h^{-1}	T, K	$w_r \times 10^3$, mol m^{-2} h^{-1}	T, K	$w_r \times 10^3$, mol m^{-2} h^{-1}
523	98.23	523	30.67	523	98	523	30
583	125.33	583	37.14	573	120	573	35
633	263.89	633	45.20	623	260	623	44
683	362.12	683	53.08	673	360	673	50

Table 4. Activation energy of CO disproportionation reaction (I) on the surface of multicomponent and binary membrane alloys

Alloy	$E_a/R \times 10^{-3}$, K	E_a, kJ/mol	Alloy addition	
			transition metals, wt %	Group III metals, wt %
B1	5.9 ± 0.2	49.2 ± 2.0	0.6 Pt–0.6 Ru	0.24Al
B2	5.6 ± 0.4	46.7 ± 3.3	–	1.5In–0.5Y
B3-1	11.4 ± 0.3	95.0 ± 2.5	0.5 W	1.5In–0.2Y
B3-2 ($\tau \le 40$ s)	1.8 ± 0.04	15.0 ± 0.3	0.5 Ta	1.5In–0.2Y
B3-3	10.5 ± 0.3	87.4 ± 2.5	0.5 Nb	1.5In–0.2Y
B3-4	5.5 ± 0.2	46.2 ± 1.7	0.5 Mo	1.5In–0.2Y
Pd–(6–10) Ru	2.14	17.90	6–10 Ru	–
Pd–5.5 Ni	1.07	8.95	5.5 Ni	–

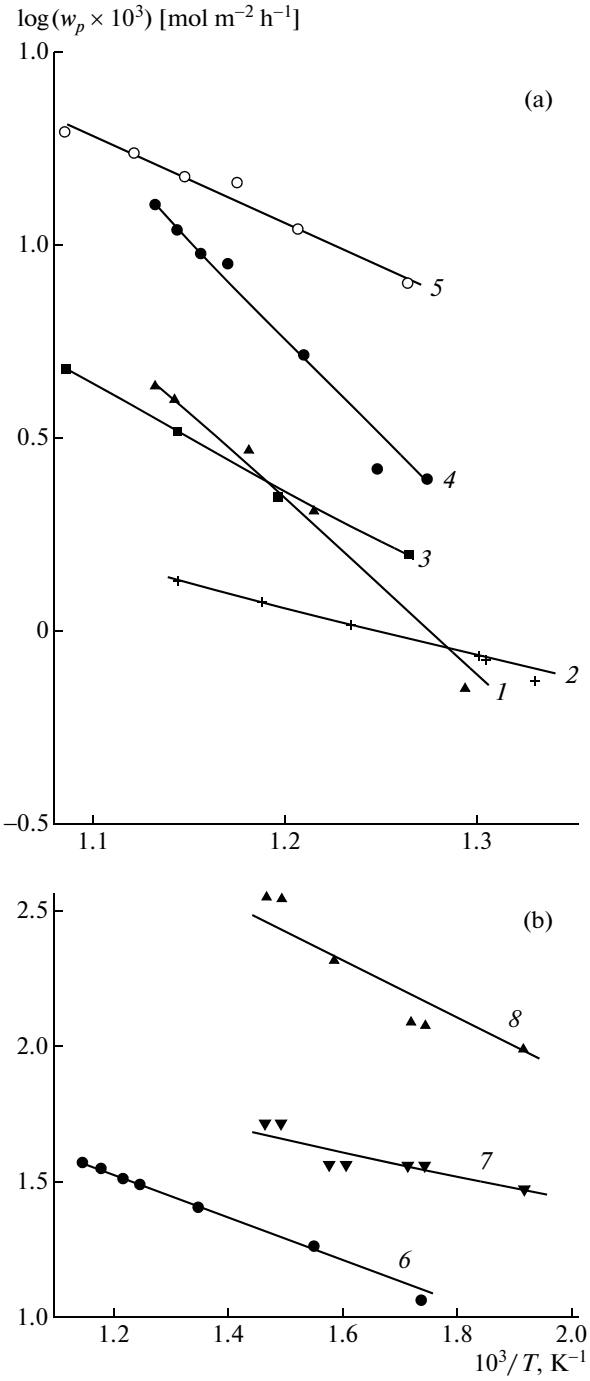

Fig. 2. The temperature dependence of the specific reaction rate of CO disproportionation on alloys in the Arrhenius coordinates (lines); points refer to experimental data for the following alloy samples: (*1*) B3-3, (*2*) B1, (*3*) B3-4, (*4*) B3-1, (*5*) B2, (*6*) B3-2, (*7*) Pd–5.5Ni, and (*8*) Pd–10Ru.

parameters (Table 1) allowed us to evaluate the disproportionation reaction conditions on multicomponent alloys with consideration for the effect of diffusion mass transfer. For this purpose, in accordance with a published method [15, 16], we calculated the ratios of

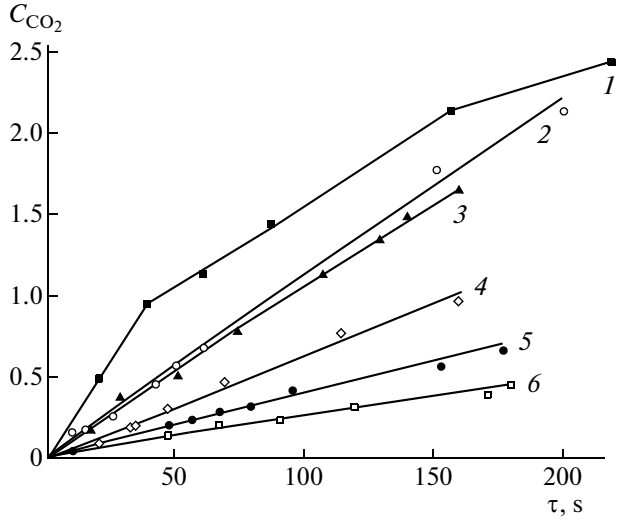

Fig. 3. Dependence of the concentration C_{CO_2} on the residence time with the surfaces of the following alloys: (*1*) B3-2, (*2*) B3-1, (*3*) B2, (*4*) B1, (*5*) B3-3, and (*6*) B3-4.

reaction rate coefficients to the coefficients of the mass transfer of CO molecules to the surface of alloys over the entire test temperature range:

$$\{w_r S_{alloy}/(V_r - V_{alloy})C_{CO}\}/\{D_{dif}S_e/(V_r - V_{alloy})\delta\} \leq (0.5-11)\times 10^{-6}, \quad (3)$$

where $D_{dif}(T = 573–925\ \text{K}) = (0.70–1.54)\times 10^{-4}\ \text{m}^2/\text{s}$ is the diffusion coefficient of CO molecules in a gas flow [17]; δ is the thickness of a boundary layer on the samples. In the case of B1 alloy, to obtain an upper estimate from relationship (3), δ was taken to be approximately equal to the diameter of samples ($\delta \leq 0.25 \times 10^{-2}$ m) at the uniform reactor filling of about 50%. For the other alloys (B2, B3) whose filling was no higher than 5%, the overall mass transfer to the surface of all of the samples was estimated. In this case, the boundary layer thickness was $\delta \leq (0.2–0.3)\times 10^{-2}$ m. From estimates obtained using relationship (3), it follows that the diffusion mass-transfer coefficient was higher than the reaction rate coefficient of disproportionation by five or six orders of magnitude for all of the samples over the entire test range of parameters. Consequently, the gas-phase diffusion of CO molecules to the surface of alloys did not limit the rate of disproportionation, which occurred in the kinetic region for all of the test membrane alloys over the entire test range of parameters. Thus, the rate of disproportionation is independent of the gas flow rate in the reactor. Indeed, differences between the rates of reaction and the average rates of reaction given in Table 2 do not exceed the relative errors of measurements for all of the alloys other than B3-2. Therefore, the deviations of particular points from average values greater than the doubled dispersion σ^2 can be due to only random errors, and they were excluded in the cal-

Table 5. Rate of formation (w_C) and the specific ($Q_C t_{exp}$) and total ($Q_C t_{exp} S_{alloy}$) yields of atomic carbon in the disproportionation of CO on the surface of membrane alloys in a maximum exposure time ($t_{exp} = 12$ h) in experiments performed at $T = 873$ K and $p = 0.105$ MPa

Alloy	$w_C \times 10^{-14}$, atom cm^{-2} s^{-1}	$Q_C t_{exp} \times 10^{-18}$, atom/cm^2	$Q_C t_{exp}$, mg/cm^2	$Q_C t_{exp} S_{alloy}$, mg
B1	0.26	1.10	0.023	9.10
B2	2.60	11.20	0.230	7.38
B3-1	2.10	9.10	0.182	11.20
B3-3	0.68	2.94	0.059	3.68
B3-4	0.51	2.20	0.044	2.57
B3-2	5.10	22.00	0.450	26.00

culation of the average values of reaction rates on B1 and B3-1 alloys. The rates of reaction on B1, B2, B3-1, B3-3, and B3-4 alloys did not depend on the flow rate of CO, and the concentrations of CO_2 molecules at the reactor outlet monotonically increased as the residence time was increased (Fig. 3).

A monotonic decrease in the rate of reaction beyond the limits of relative errors (±10%) was detected in B3-2 alloy as the flow rate of CO was decreased (Table 2). In this case, deviations from the arithmetic mean value of the rate of reaction at all points ($n = 6$) were greater than 70%, and σ^2 was higher than the average value by a factor of 5. At the same time, on this alloy, which is characterized by a maximum rate of reaction at residence times $\tau \le 40$ s, a break of a curve was detected in the dependence of the concentration of CO_2 on residence time (Fig. 3). As shown above, this break cannot be explained by reaction rate limitations due to diffusion mass transfer. Moreover, after the experiments performed at the constant temperature $T = 873$ K, the residence times $\tau >$ 40 s, and the exposure t_{exp} ~12 h, a continuous transparent violet film was detected on the surface of B3-2 alloy; this film was easily removed upon sample bending. The violet color was due to the interference of incident and reflected light; it suggests that the film thickness was about the wavelength of this light (~350–400 nm). Undoubtedly, the formation of this film was responsible for an almost twofold decrease in the rate of reaction as the film thickness increased over the residence time interval $\tau = 60$–200 s (Fig. 3) by blocking the alloy surface.

The formation of polymer films on the surfaces of other alloys was not observed. After the experiments at $T = 873$ K and exposure times to 12 h in a flow of CO, only a barely perceptible dark carbon deposit was detected on the surfaces of B2 and B3-1 alloys; this deposit was easily removed from the surface with a flow of air. Therefore, carbon did not exhibit strong adhesion to the alloy surface and to individual carbon particles. The absence of chemical bonds clearly indicated that the detected deposit was different from pyrolytic carbon. It can be a deposit of soot or graphite particles.

In disproportionation reaction (I), the yield of carbon atoms is equal to the yield of CO_2 molecules. This allowed us to calculate the specific and total yields of carbon, which resulted from reaction (I) on the surfaces of various alloys at $T = 873$ K during the maximum time of measurements ($t_{exp} = 12$ h) (Table 5), from data in Table 2.

From these data, it follows that the amount of carbon atoms formed on the alloy surfaces in the experiment times as a result of the reaction was sufficient for the formation of deposits from 335 to 680 nm in thickness at distances between carbon layers characteristic of graphite (0.335 nm) and soot particles. They can completely block the surface and decrease the rate of reaction to its termination. However, even a monotonic decrease in the reaction rate with exposure time was not detected on the alloys other than B3-2 alloy. At the same time, a continuous polymer film 350–400 nm in thickness formed on the surface of B3-2 alloy incompletely blocked the surface. The molecules of CO continued to arrive at the alloy surface from a gas phase and enter into reaction (I); this suggests the occurrence of the diffusion of CO molecules and the release of the resulting gas-phase products through the polymer film.

Therefore, the average reaction rate of CO disproportionation on B3-2 alloy (Table 2) was calculated from the points that corresponded to the rates $Q_{CO} \ge$ 0.0140 mol/h and residence times $\tau \le 40$ s, at which the formation of a polymer film was not detected. The activation energy of reaction on this alloy was also calculated at $\tau = 40$ s in the absence of a film on the surface.

An analysis of these data, especially, small amounts of carbon deposits and weak bonds to the surfaces of B2 and B3-1 alloys, where the rates of reaction were much higher than on the other alloys (B1, B3-3, and B4), led us to a conclusion that the surface was continuously cleaned from carbon removed with a gas flow in the course of reaction on all of the membrane alloys other than B3-2 alloy.

DISCUSSION

Let us consider a possible mechanism of heterogeneous reaction (I) based on the above experimental data (Tables 2–5, Fig. 3) and the results of a study of the structure and bond energies of CO molecules adsorbed on the surface of Group VIII metals [18] and Pd–Ru membrane alloys [7–9, 14] using various techniques.

The experimental data demonstrate the occurrence of heterogeneous reaction (I) on all of the membrane alloys. In this case, the change in the average concentration of CO molecules in a gas phase along the reactor was lower than 2–5% in the course of reaction on all of the alloys at a constant temperature. Consequently, all of the active surface sites on all of the alloys were permanently occupied by adsorbed particles over the entire test ranges of residence times and temperatures. From the experimental data (Tables 2, 3), it follows that the rate of reaction and hence the composition and structure of sites active in reaction (I) and the concentrations of particles adsorbed on them depend on temperature and alloy composition and do not depend on residence time.

It is well known that the adsorption of CO molecules on all of the Group VIII metals [18] and the test palladium membrane alloys [7–9] occurrs at active sites of two types to form weak and strong bonds, respectively. The weak bond occurred in the reversible low-temperature adsorption at one active site, and it was characterized by the linear structure of an adsorption complex, whereas the strong one occurred in the irreversible dissociative adsorption with the formation of a bridging structure due to the bond of CO molecules with two or more active sites of different types [7–9, 14].

Thus, two forms of adsorption with maximums at 690 ± 10 and 960 ± 30 K were detected on the surface of a binary PdRu membrane alloy by thermal desorption from the surface presaturated with CO molecules at $T = 773$–973 K. On desorption from the surface presaturated with CO molecules at lower temperatures $T \leq 523$ K, only one peak at 690 ± 20 K was detected; this peak shifted to 720 K and broadened to 1000 K as the adsorption temperature was increased to 573 K [7]. Both of the peaks were detected upon cooling from 773 to 295 K in a continuous flow of CO [14, 19]. In the presence of a single peak, only CO molecules were detected in thermal desorption products, whereas CO and CO_2 molecules were detected upon the appearance of a second peak in the thermal desorption spectra [7]. These data allowed us to relate first type sites s_1 (peak at 690 K) to the reversible adsorption–desorption of CO molecules and second type sites s_2 to the dissociative adsorption of CO (peak at 960 K) [7, 14] because the presence of a peak at 960 K is a necessary condition for the formation of CO_2.

The dissociative adsorption of CO cannot occur with the participation of only one site because of the great molecular dissociation energy (1066 kJ/mol) [20], which is higher than the atomic bond energies in MO (486–1063 kJ/mol) and MC crystals (611–1237 kJ/mol) in the majority of the test membrane alloys [21]. Therefore, it is most likely that the dissociation of CO molecules results from irreversible adsorption at two or more closely spaced alloy metal atoms, which comprise an active site s_2 with the formation of adsorbed Cs_2' and Os_2'' atoms on the surface. The multicenter dissociative and one-center reversible forms of the adsorption of CO and hydrogen molecules were detected on the surfaces of all of the Group VIII metals [18] and PdRu and PdNi binary alloys [7, 14].

Similar low-temperature and high-temperature adsorption sites will occur on the surfaces of other binary and multicomponent membrane palladium alloys, in particular, alloys from the series B1–B3, because their constituents are addition elements of Group I (Ag and Au), Group III (Al, In, and Y), Group V (Ta and Nb), Group VI (Mo and W), and Group VIII (Ru and Pt) metals, which possess high catalytic properties, in addition to palladium (Table 4).

Based on the above analysis of the experimental results and published data, we suggest that the probable mechanism of CO_2 formation in a flow of CO on the test multicomponent membrane palladium alloys from the series B1–B3, as well as on membrane PdRu and PdNi binary alloys, involves the following steps:

$$CO + s_1 \longleftrightarrow COs_1, \quad \text{(IV)}$$

$$CO + s_2 \longrightarrow (COs_2)^* \longrightarrow Cs_2' + Os_2'', \quad \text{(V)}$$

$$COs_1 + Os_2'' \longrightarrow (CO_2)^*s_2'' + s_1, \quad \text{(VI)}$$

$$CO + Os_2'' \longrightarrow (CO_2)^*s_2'', \quad \text{(VII)}$$

$$(CO_2)^*s_2'' \longrightarrow CO_2\uparrow + s_2'', \quad \text{(VIII)}$$

where s_1 are the low-temperature sites of reversible adsorption and s_2 are the high-temperature sites of dissociative (irreversible) adsorption of CO, and, s_2'' and s_2' are the portions of multicomponent s_2 sites. It is different from the mechanism of thermal adsorption followed by vacuum desorption [7] only in the presence of possible step (VII) [14].

At low temperatures ($T < 573$ K), only the reversible adsorption of CO occurred to result, in combination with the reverse reaction, desorption (IV), in an equilibrium at this step. As the temperature was increased ($T \geq 573$ K), the irreversible adsorption of CO molecules at active sites of the second type was detected; it resulted in dissociation (V) with the formation of equal amounts of oxygen and carbon atoms adsorbed at different parts of these sites Cs_2' and Os_2''. The bond energies of adsorbed oxygen and carbon atoms at Group VIII metals (Pd, Pt, Ru, and Ni) and, probably, other transition metals were 260–420 and 80–160 kJ/mol, respectively [18]. Subsequently, the

adsorbed oxygen atoms were completely consumed in reactions (VI)–(VII) for the formation of CO_2 molecules, which were desorbed from the surface into a gas flow (VIII). As a result of reactions (VI)–(VIII), the s_1 and s_2'' surface sites were purified.

Carbon atoms remained as Cs_2' at the surface sites. Their subsequent behavior depended on the character and strength of bonds with s_2' sites. From IR spectroscopic data, it follows that CO molecules can be adsorbed in a strongly bound bridging form in the following probable configurations:

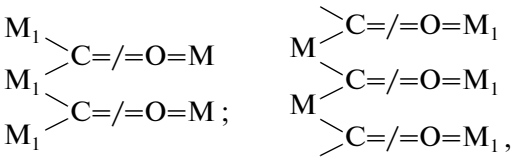

A **B** (IX)

where M and M_1 are palladium and additional element atoms, including Group VIII metals, that constituted s_2 active sites at various faces of the crystal lattice, and the / sign indicates the site of bond rupture with the formation of adsorbed Cs_2' and Os_2'' atoms. After dissociation and the interaction of adsorbed oxygen atoms with CO molecules followed by the desorption of CO_2 (VI)–(VIII), carbon atoms adsorbed at the neighboring M and M_1 metal atoms (Cs_2') in configuration **A** (IX) remained on the surfaces of alloys. It is likely that, in this configuration, neighboring carbon atoms interacted with the formation of excited $C_n^*s_2'$ molecules ($n \geq 2$). The internal excitation energies of the resulting C_2–C_8 carbon molecules (600–4100 kJ/mol [21]) was sufficient for the rupture of their bonds with two (160–320 kJ/mol) or more s_2' sites and the desorption of free carbon as a mixture of C_n molecules from the surface to a gas flow. As a result of the desorption of carbon molecules from the surface, all of the s_2' sites were liberated:

$$Cs_2' + (n-1)Cs_2' \longrightarrow C_n^*s_2' + s_2' \longrightarrow C_n\uparrow + 2\,s_2'. \quad (X)$$

The main portion of desorbed carbon molecules was removed with a gas flow, whereas a portion of heavier molecules could be deposited on the surface as a film, which was detected on the surface of the B2 and B3-1 test multicomponent membrane alloys. This deposit of carbon molecules or particles was readily removed by a flow of air after the removal of the samples into the atmosphere. The occurrence of these reactions explains the experimental fact that strong chemical bonds with the surface and between deposited carbon particles were absent from B1, B2, B3-1, B3-3, and B3-4 alloys and a polymer film was absent from the surface of B3-2 alloy. At the same time, reactions (X) resulted in the reduction of s_2 sites

$$s_2' + s_2'' \longrightarrow s_2. \quad (XI)$$

Thus, all of the active surface sites of both types, which participated in the disproportionation process, were liberated and occupied once again as a result of the subsequent dissociative and reversible adsorption of CO molecules on all of the test membrane palladium alloys. The above mechanism of reactions (IV)–(XI) explains the observed absence of changes in the reaction rate depending on the residence time of a flow of CO with the surfaces of all of the alloys other than B3-2.

In the case of B3-2 alloy, whose composition differed from that of the other alloys only in the presence of tantalum as an addition element, the Ta–C bond was the strongest, as compared with the Pd–C, Y–C, Mo–C, Nb–C, and W–C bonds, and the formation of heavier C_n molecules was required for the rupture of this bond. In this case, at least a portion of carbon atoms and molecules could be more strongly bound to the surface atoms of tantalum (M_1). The chemisorption of CO molecules and the subsequent reactions up to the formation of a polymer film, which was weakly bound to the surface, can occur at the adsorbed C_{M1} atoms or C_{nM_1} carbon molecules by the loosening of the Ta–C bond in the course of polymerization.

The violet film deposited on the surface of B2 alloy was similar to a film deposited on a glass reactor surface in the course of a study of the decomposition of CO molecules in a nonequilibrium glow-discharge plasma at reduced pressures [22]. The formation of $C(^3P)$ and $O(^3P)$ atoms as a consequence of the electron-impact dissociation of CO molecules was detected in the bulk of the plasma. In this case, the formation of a film was detected on the walls of a discharge tube. According to IR spectroscopic and X-ray diffraction data, the composition of the film, which was analogous to the film on the surface of B3-2 alloy in these experiments in appearance and color, corresponded to the $[C_xO_y]_n$ polymer, in which the x/y ratio varied from 2 : 1 to 3 : 2 and color varied from black to violet depending on the composition of the gas phase. A study of the material balance of chemical reactions occurring in the discharge demonstrated that the film formation was initiated by the deposition of carbon atoms onto the surface of molybdenum glass, and the growth propagation was due to the adsorption of CO molecules and C atoms on them from the gas phase [18].

An analogous mechanism—the subsequent adsorption of CO molecules on C atoms adsorbed at s_2 sites on the surface of B3-2 alloy with the formation of $[C_xO_y]_n$ polymers—is also possible in the disproportionation of CO.

In our opinion, the absence of coke or soot formation from the surfaces of other alloys studied in this work provides support for the above reaction mechanism with consideration for the formation of carbon molecules, the desorption of them into the gas phase, and the removal with a gas flow. Otherwise, polymer

films, coke, or soot would be formed on the surfaces of all of the alloys to affect the rate and activation energy of forward reaction (I).

An analysis of the experimental results and published data showed that the reaction rates and activation energies (E_a) reflect the desorption of CO_2 molecules over the temperature range of CO disproportionation reaction (573–925 K) on multicomponent (B1–B3) and two-component membrane Pd–10Ru and Pd–5.5Ni palladium alloys [7]. According to the above disproportionation mechanism of reactions (IV)–(XI), these results reflect the temperature distribution of the concentrations of active surface sites (s_2) of the strong bridging form of the adsorption of CO molecules for corresponding alloys [7, 18].

At gas pressure $p \geq 0.1$ MPa, the formation of CO_2 resulted from consecutive reactions: dissociative CO adsorption (VI) with the formation of Os_2 adsorbed oxygen atoms followed by the oxidation of CO molecules adsorbed at other sites s_1 (V) or immediately at Os_2 atoms (VII). One way or the other, all of these steps occurred at the active sites of alloy surfaces. At a gas pressure of 0.1 MPa in the reactor and $T = 873$ K, the flow of CO molecules to the surface of alloy samples was 3×10^{24} molecule $cm^{-2}\ s^{-1}$. Therefore, the adsorption surface sites s_1 and s_2 should be completely occupied by CO molecules with the formation of adsorbed Os_2'' and Cs_2' atoms in a time shorter than 3×10^{-6} s [23, 24]. From the experimental data, it follows that Os_2'' atoms decayed in the reactions of CO_2 formation with a characteristic time of no shorter than 10 s (Fig. 3). Thus, the oxidation of CO by the interaction with adsorbed oxygen atoms is the rate-limiting step of the reaction of CO_2 formation. An increase in the reactor pressure above 0.1 MPa and in the flux of CO molecules to the alloy surfaces cannot affect the rates of CO oxidation steps and the formation of CO_2 molecules with their desorption into a gas phase because the purification of s_2' sites and the regeneration of s_2 active sites occurred only after the formation and desorption of CO_2 and C_n molecules. Consequently, the rate of CO disproportionation reaction (I) is independent of gas pressure. The absence of the pressure dependence of the rate of the reaction was also supported by published experimental data [7–9].

Based on the above consideration, we can make the following conclusions:

(1) The specific rate of reaction (w_r) of CO disproportionation with the formation of CO_2 molecules and Cs_2' adsorbed atomic carbon is independent of the residence time of CO with the surfaces of all of the test multicomponent membrane palladium alloys other than B3-2. At $T = 833$–925 K, w_r decreases in the order B3-2 ⟶ B2 ⟶ B3-1 ⟶ B3-3 ⟶ B3-4 ⟶ B1. At the same process parameters, it was lower than that on two-component membrane alloys: at least by one order of magnitude, as compared with PdRu alloy, or by a factor of more than 2–3, as compared with PdNi alloy.

(2) The reaction rate of disproportionation monotonically decreased with decreasing temperature on all of the test multicomponent and two-component membrane palladium alloys. The change in the activation energy of the reaction on palladium alloys with various compositions ($E_a = 9$–95 kJ/mol) reflects the shape of the temperature distribution of the concentration of s_2 active sites, which depends on the nature and concentration of alloy elements.

(3) The formation of atomic carbon in the reaction of CO disproportionation on all of the test membrane palladium alloys other than B3-2 does not result in the formation of coke or soot deposits, which can decrease the rate of reaction at residence times to 200 s and total exposure times to 12 h, on their surfaces.

(4) On the surface of B3-2 alloy, atomic carbon adsorbed as a result of the reaction initiates the formation of a polymer film, which is weakly bound to the surface but partially blocks it to cause a monotonic decrease in the rate of reaction over the residence time range of 40–200 s by a factor of almost 2. The reaction rate and activation energy for this alloy were determined at the CO residence time with the surface $\tau =$ 40 s in the absence of a film.

(5) We proposed a reaction mechanism to adequately explain the experimental results.

REFERENCES

1. Slovetskii, D.I., *Drag. Kamni Drag. Met.*, 2003, no. 1, p. 119.
2. Knapton, A.G., *Platinum Met. Rev.*, 1977, vol. 21, p. 44.
3. German Patent 2305595, 1974.
4. Mordkovich, V.Z., Baichtock, Yu.K., and Sosna, M.H., *Platinum Met. Rev.*, 1992, vol. 36, p. 90.
5. Tarasova, V.E. and Pavlova, L.F., in *Metally i splavy kak membrannye katalizatory* (Metals and Alloys As Membrane Catalysts), Gryaznov, V.M. and Klabunovskii, E.I., Eds., Moscow: Nauka, 1981, p. 120.
6. Roshan, N.R. and Polyakova, V.P., in *Metallicheskie monokristally* (Metal Single Crystals), Moscow: Nauka, 1990, p. 235.
7. Gur'yanova, O.S., Serov, Yu.M., Lapidus, A.L., Dmitriev, R.G., Gul'yanova, S.G., Gryaznov, V.M., and Minachev, Kh.M., *Izv. Akad. Nauk SSSR, Ser. Khim.*, 1987, no. 11, p. 2428.
8. Gur'yanova, O.S., Serov, Yu.M., Gul'yanova, S.G., and Gryaznov, V.M., *Kinet. Katal.*, 1988, vol. 29, no. 4, p. 850.
9. Gryaznov, V.M., Gul'yanova, S.G., and Serov, Yu.M., *Usp. Khim.*, 1989, vol. 58, p. 58.
10. Koshel', V.I., Dobradin, A.A., and Chistov, E.M., *Vestn. Akad. Nauk BSSR, Ser. Fiz. Energ. Nauk*, 1983, no. 2, p. 102.

11. Rozovskii, A.Ya. and Lin, G.I., *Teoreticheskie osnovy protsessa sinteza metanola* (Theoretical Foundations of Methanol Synthesis), Moscow: Khimiya, 1987, p. 74.

12. Rapoport, F.M. and Il'inskaya, A.A., *Laboratornye metody polucheniya chistykh gazov* (Laboratory Methods of Preparation of Pure Gases), Moscow: Goskhimizdat, 1963, pp. 44–45, 238–242.

13. Gol'tsov, V.A., Latyshev, V.V., Timofeev, N.I., and Machikina, N.Yu., *Izv. Vyssh. Uchebn. Zaved., Tsvetn. Metall.*, 1977, no. 4, p. 117.

14. Serov, Yu.M., *Doctoral (Chem.) Dissertation*, Moscow: Peoples' Friendship University of Russia, 1999, p. 28.

15. Boreskov, G.K., *Kataliz v proizvodstve sernoi kisloty* (Catalysis in Sulfuric Acid Production), Moscow: Goskhimizdat, 1954, p. 71.

16. Boreskov, G.K., *Geterogennyi kataliz* (Heterogeneous Catalysis), Moscow: Nauka, 1988, pp. 233–248.

17. Dubovkin, N.F., *Spravochnik po uglevodorodnym toplivam i ikh produktam sgoraniya* (Handbook of Hydrocarbon Fuels and Their Combustion Products), Moscow: Gosenergoizdat, 1962.

18. Popova, N.M., Babenkova, L.V., and Savel'eva, G.A., *Adsorbtsiya i vzaimodeistvie prosteishikh gazov s metallami VIII gruppy* (Adsorption and Interaction of the Simplest Gases with Group VIII Metals), Alma-Ata: Nauka, 1979.

19. Serov, Yu.M., Gryaznov, V.M., and Gul'yanova, S.G., *Izv. Vyssh. Uchebn. Zaved., Khim. Khim. Tekhnol.*, 1981, vol. 24, no. 3, p. 321.

20. Vedeneev, V.I., Gurvich, L.V., Kondrat'ev, V.N., Medvedev, V.A., and Frankevich, E.L., *Energii razryva khimicheskikh svyazei: Spravochnik* (Bond Dissociation Energies: A Handbook), Moscow: Akad. Nauk SSSR, 1962.

21. *Termicheskie konstanty veshchestv: Spravochnik* (Thermal Constants of Substances: A Handbook), Moscow: Akad. Nauk SSSR, 1979, issues V–VIII.

22. Slovetskii, D.I., *Khimiya plazmy* (Plasma Chemistry), Moscow: Energoatomizdat, 1984.

23. Mikhalenko, I.I. and Yagodovskii, V.D., *Kinet. Katal.*, 2004, vol. 45, no. 2, p. 256 [*Kinet. Catal.* (Engl. Transl.), vol. 45, no. 2, p. 239].

24. Mikhalenko, I.I., Chernova, A.E., Roshan, N.R., Chistov, E.M., and Slovetskii, D.I., *Materialy mezhd. nauch. konf. po nestatsionarnye energo- i resursosberegayushchie protsessy i oborudovanie v khimicheskoi, nano- i biotekhnologii* (Proc. Int. Conf. on Unsteady-State Energy- and Resource-Saving Processes and Equipment for Chemical Technology, Nanotechnology, and Biotechnology), Moscow, 2008, p. 174.